


# Comparative analysis of thymic subpopulations during different modes of atrophy identifies the reactive oxygen species scavenger, *N*-acetyl cysteine, to increase the survival of thymocytes during infection-induced and lipopolysaccharide-induced thymic atrophy

Shamik Majumdar,<sup>1</sup> Vasista Adiga,<sup>2</sup>  
Abinaya Raghavan,<sup>1</sup> Supriya  
Rajendra Rananaware<sup>1</sup> and  
Dipankar Nandi<sup>1,2</sup> 

<sup>1</sup>Department of Biochemistry, Indian Institute of Science, Bangalore, and <sup>2</sup>Centre for Infectious Disease Research, Indian Institute of Science, Bangalore, India

## Summary

The development of immunocompetent T cells entails a complex pathway of differentiation in the thymus. Thymic atrophy occurs with ageing and during conditions such as malnutrition, infections and cancer chemotherapy. The comparative changes in thymic subsets under different modes of thymic atrophy and the mechanisms involved are not well characterized. These aspects were investigated, using mice infected with *Salmonella* Typhimurium, injection with lipopolysaccharide (LPS), an inflammatory but non-infectious stimulus, etoposide (Eto), a drug used to treat some cancers, and dexamethasone (Dex), a steroid used in some inflammatory diseases. The effects on the major subpopulations of thymocytes based on multicolour flow cytometry studies were, first, the CD4<sup>-</sup> CD8<sup>-</sup> double-negative (DN) cells, mainly DN2–4, were reduced with infection, LPS and Eto treatment, but not with Dex. Second, the CD8<sup>+</sup> CD3<sup>lo</sup> immature single-positive cells (ISPs) were highly sensitive to infection, LPS and Eto, but not Dex. Third, treatment with LPS, Eto and Dex reduced all three subpopulations of CD4<sup>+</sup> CD8<sup>+</sup> double-positive (DP) thymocytes, i.e. DP1, DP2 and DP3, but the DP3 subset was relatively more resistant during infection. Fourth, both CD4<sup>+</sup> and CD8<sup>+</sup> single-positive (SP) thymocytes were lowered by Eto and Dex, but not during infection. Notably, LPS lowered CD4<sup>+</sup> SP subsets, whereas the CD8<sup>+</sup> SP subsets were relatively more resistant. Interestingly, the reactive oxygen species quencher, *N*-acetyl cysteine, greatly improved the survival of thymocytes, especially DNs, ISPs and DPs, during infection and LPS treatment. The implications of these observations for the development of potential thymopoietic drugs are discussed.

**Keywords:** infection; lipopolysaccharide; reactive oxygen species; thymic atrophy; thymocyte subpopulations.

doi:10.1111/imm.13043

Received 28 September 2018; revised 7  
December 2018; accepted 10 January 2019.

Correspondence: Dipankar Nandi, FE-14,  
Biochemistry Department, Biological  
Sciences Building, Indian Institute of  
Science, Bangalore 560012, India.

Email: nandi@iisc.ac.in

Senior author: Dipankar Nandi

## Introduction

T cells are an indispensable component of the adaptive immune system. Progenitor cells arising from the bone

marrow undergo sequential development and selection in the thymus, a primary lymphoid organ, to give rise to immunocompetent T cells. Thymocytes can be broadly classified into four developmental stages on the basis of

Abbreviations: CFU, colony-forming units; DEX, dexamethasone; DN, double-negative; DP, double-positive; ETO, etoposide; GCs, glucocorticoids; IFN- $\gamma$ , interferon- $\gamma$ ; IL-6, interleukin-6; ISP, immature single-positive; LPS, lipopolysaccharide; MFI, median fluorescence intensity; NAC, *N*-acetyl cysteine; nd, not detected; NE, no effect; ns, not significant; PBS, phosphate-buffered saline; ROS, reactive oxygen species; *S. Typhimurium*/ST, *Salmonella* Typhimurium; SP, single-positive; TCR, T-cell receptor; TNF- $\alpha$ , tumour necrosis factor- $\alpha$ ; UT, untreated

cell-surface expression of the T-cell co-receptors CD4 and CD8. The CD4<sup>-</sup> CD8<sup>-</sup>, i.e. double-negative (DN), cells are the most immature. These cells proliferate and give rise to the CD4<sup>+</sup> CD8<sup>+</sup>, i.e. double-positive (DP), cells, where they undergo selection, after which the DP cells generate either the CD4<sup>+</sup> CD8<sup>-</sup> or the CD4<sup>-</sup> CD8<sup>+</sup>, i.e. single-positive (SP), cells. In recent years, additional developmental and maturation markers on thymocytes have been discovered, which has led to the study of subpopulations of thymocyte subsets. In the DN subset, surface expression of CD44 and CD25 define four distinct developmental stages: DN1 (CD4<sup>-</sup> CD8<sup>-</sup> CD44<sup>+</sup> CD25<sup>-</sup>), DN2 (CD4<sup>-</sup> CD8<sup>-</sup> CD44<sup>+</sup> CD25<sup>+</sup>), DN3 (CD4<sup>-</sup> CD8<sup>-</sup> CD44<sup>-</sup> CD25<sup>+</sup>) and DN4 (CD4<sup>-</sup> CD8<sup>-</sup> CD44<sup>-</sup> CD25<sup>-</sup>).<sup>1</sup> The DN4 cells produce the DP cells through an intermediate Notch-dependent stage, called the immature single-positive (ISP) cells, which are phenotypically characterized as CD4<sup>-</sup> CD8<sup>+</sup> CD3<sup>lo</sup> CD24<sup>hi</sup>. The DP cells, generated from the ISP cells, can be developmentally fractionated into three stages: DP1 (CD4<sup>+</sup> CD8<sup>+</sup> CD5<sup>lo</sup> CD3<sup>lo</sup>), DP2 (CD4<sup>+</sup> CD8<sup>+</sup> CD5<sup>hi</sup> CD3<sup>int</sup>) and DP3 (CD4<sup>+</sup> CD8<sup>+</sup> CD5<sup>int</sup> CD3<sup>hi</sup>). The DP1 cells are the preselected thymocytes, which exclusively produce the DP2 cells that give rise to either the DP3 cells or cells of the CD4 lineage. On the other hand, the DP3 cells are restricted to generate only the CD8<sup>+</sup> SP cells.<sup>2</sup> Numerous markers including CD24 and CD3<sup>3</sup> and CD69 and CD62L<sup>4</sup> have been used to study the SP cells at different stages of maturation. For example, the CD24<sup>hi</sup> CD3<sup>hi</sup> and CD24<sup>int</sup> CD3<sup>hi</sup> cells are the more immature cells in the SP subset, whereas the CD24<sup>lo</sup> CD3<sup>hi</sup> are comparatively more mature.<sup>5</sup> Naive CD4<sup>+</sup> and CD8<sup>+</sup> T cells egress the thymus after maturation of SPs. The output and fitness of the thymus is quantified by the export of naive T cells into the circulation.

The thymus is extremely sensitive to stress and atrophies readily during numerous conditions including ageing. Thymic atrophy, i.e. the loss in cellularity of the thymus, is observed during conditions such as malnutrition, infections, chemotherapy and stress in both mice and humans.<sup>6</sup> In majority of cases, thymic atrophy is accompanied by loss in architecture of the thymus and reduction in its output. To study the process of thymic atrophy and its underlying mechanisms, numerous mouse models of thymic atrophy have been standardized. Viral, bacterial and parasitic infections often accompany thymic atrophy.<sup>7</sup> Whole pathogens or microbial components can also cause thymic atrophy. Intraperitoneal injection of *Escherichia coli* leads to significant loss of the DN and DP populations, while the cellularity of the SP subsets is unaffected. This process is dependent on tumour necrosis factor- $\alpha$  (TNF- $\alpha$ ) and inhibition of protein synthesis.<sup>8</sup> Lipopolysaccharide (LPS) is a major microbial component that leads to endotoxic shock-induced thymic

atrophy. Acute thymic atrophy in terms of both weight and cellularity of the thymus occurs upon intraperitoneal injection of LPS in mice. Up-regulation of genes involved in inflammation and wound healing/tissue modelling occurs, while genes involved in T-cell development, cell activation and cell cycle progression are down-regulated.<sup>9</sup> C3H/HeJ mice, which lack *Tlr4*, display reduced thymic atrophy compared with their Toll-like receptor 4-sufficient counterparts, C3H/HeN mice.<sup>10</sup> During LPS-induced thymic atrophy, thymic levels of leukaemia inhibitory factor, a member of the interleukin-6 (IL-6) cytokine family, increase and become functionally important.<sup>11</sup>

Chemotherapeutic drugs used to treat cancer also induce transient thymic atrophy.<sup>12,13</sup> For example, etoposide (Eto) forms complexes with topoisomerase II and DNA and inhibits re-ligation of the DNA strands, thereby inducing DNA breaks and leading to apoptosis of thymocytes.<sup>14</sup> Eto induces nitric oxide in rat thymocytes and causes apoptosis by caspase activation.<sup>15</sup> In addition, Eto-induced apoptosis can be prevented by pre-treatment of thymocytes with a protein synthesis inhibitor<sup>16</sup> or with an inhibitor of proteasomes.<sup>17</sup>

Glucocorticoids (GC), steroid hormones secreted primarily by the adrenal glands, occupy a central position in mediating thymic atrophy in mice during various conditions. Importantly, GCs are used to treat several inflammatory diseases, e.g. autoimmune diseases and allergies. To study the mechanisms of GC-induced thymocyte death, the synthetic GC analogue, dexamethasone (Dex) has been extensively used. It induces phosphorylation of phosphatidylinositol-specific phospholipase C and ceramide generation. Consequently, caspase-3, caspase-8 and caspase-9 are activated along with cytochrome c release from the mitochondria, culminating in apoptosis of thymocytes.<sup>18</sup> Dex induces apoptosis of rat thymocytes in both G0/G1 and G2/M phases of the cell cycle.<sup>14</sup> Accordingly, adrenalectomy or inhibition of action of GCs using GC receptor antagonists such as RU486, reduce thymic atrophy during infections,<sup>19–23</sup> LPS administration<sup>24,25</sup> and cancer.<sup>26,27</sup>

In spite of the phenomenon of thymic atrophy being widely studied in mouse models, comparative and detailed investigations on the major thymocyte subpopulations have not been performed. Our laboratory has studied distinct infection-induced changes occurring in the major thymocyte subpopulations during *Salmonella* Typhimurium infection-induced thymic atrophy in C57BL/6 mice.<sup>5</sup> The broad questions that we asked in this study were whether there are differences in subpopulations during various modes of thymic atrophy, namely, treatments with LPS (inflammatory but non-infectious), Eto (drug used to treat different cancers) and Dex (clinically used to treat several inflammatory diseases) in BALB/c mice, using multicolour flow cytometry. The

S. Typhimurium-induced thymic atrophy model (inflammatory and infectious) previously standardized in our laboratory<sup>5,23</sup> served as a useful control. Distinct differences were observed in the thymocyte subpopulations in all the thymic atrophy models studied. In addition, the roles of reactive oxygen species (ROS) in mediating the observed changes were subsequently investigated. The potential of ROS quenchers as a thymopoietic drug has also been discussed.

## Materials and methods

### Bacterial cultures

Oral infections in BALB/c mice were performed using the S. Typhimurium strain NCTC 12023.<sup>23</sup> The glycerol stocks of the bacteria were revived in 3 ml of Luria broth and the culture was streaked on a *Salmonella-Shigella* agar plate. A single isolated colony from a *Salmonella-Shigella* agar plate was inoculated in 3 ml of Luria broth, which was grown for 8 hr at 37° and 160 rpm. This pre-inoculum was added at 0.05% in 50 ml of Luria broth. The cells were cultured for 3–5 hr to obtain bacterial cells in the log phase. The cells were washed in phosphate-buffered saline (PBS) and the optical density was measured. The mice were given ~10<sup>9</sup> colony forming units (CFU) of S. Typhimurium/mouse by oral gavage.<sup>23</sup>

### Mouse infections and reagents

All experiments were performed in 6- to 8-week-old male BALB/c mice. The mice were bred and maintained at the Central Animal Facility of the Indian Institute of Science (IISc), Bangalore. Unless otherwise stated, the reagents used in this study were obtained from Sigma-Aldrich (St Louis, MO). Eto (E1383-100MG) and Dex (Dexona, Cadila Health Ltd, Ahmedabad, India) were dissolved in dimethylsulphoxide, while LPS (L2630-25MG) was solubilized in PBS. Dose titration studies were performed and the compounds were intraperitoneally administered to mice at the indicated doses. N-acetyl-L-cysteine (NAC) (A9165-25G) was dissolved in PBS and was given by oral gavage 16 and 32 hr after infection/treatment.

### Ethics statement

All experiments were designed and performed upon approval and were in accordance with the Control and Supervision rules, 1998 of the Ministry of Environment and Forests Act (Government of India) and Institutional Animal Ethics Committee, IISc guidelines. Breeding and maintenance of mice were conducted at the Central Animal Facility of IISc (Registration number: 48/1999/CPCSEA, dated 1/3/1999) upon approval by the Ministry of Environment and Forests, Government of India. In addition, the

experimental protocols were approved by the 'Committee for Purpose and Control and Supervision of Experiments on Animals', with the permit number being CAF/Ethics/216/2011. Details of the national guidelines are available on: <http://envfor.nic.in/division/committee-purpose-control-and-supervision-experiments-animals-cpcsea>.

### CFU analysis

The mice on the mentioned days post-infection were killed and the organs were harvested and collected in PBS. The organs were weighed and homogenized in 1 ml PBS and the appropriate dilutions were plated on *Salmonella-Shigella* agar plates. The plates were incubated at 37° for 12–16 hr and the black-centred bacterial colonies were enumerated.<sup>23</sup>

### Isolation of thymocytes

The mice were killed on the indicated days and the thymi were harvested and collected in RPMI medium supplemented with 5% fetal bovine serum (Gibco, Gaithersburg, MD). The organs were gently disrupted using a pair of forceps and the cell suspensions were passed through a fine wire mesh to obtain single-cell suspensions. The viable cell numbers were calculated using a Trypan blue exclusion assay with the help of a haemocytometer.<sup>23</sup>

### Quantification of cytokines and cortisol

The mice were killed and blood was collected by cardiac puncture. Blood was allowed to clot at 4° to enable collection of sera. Serum TNF- $\alpha$ , IL-6 and interferon- $\gamma$  (IFN- $\gamma$ ) amounts were quantified using ELISA kits (Thermo Fisher Scientific, Waltham, MA), while the serum cortisol amounts were estimated using the Accu-Bind ELISA kit (Monobind Inc., Lake Forest, CA) according to the manufacturer's instructions.<sup>23</sup>

### Flow cytometric analysis

The various cell populations in the thymi were studied using multicolour flow cytometry. The panel of antibodies used to analyse the thymocyte subpopulations were standardized in a previous study from our laboratory.<sup>5</sup> Briefly, the thymocytes were kept for 45 min at 4° with the mentioned antibodies specific to cell-surface markers. Subsequently, the samples were washed and fixed with 0.5% paraformaldehyde before acquisition on the BD Verse™ flow cytometer. The baseline autofluorescence and compensation settings for each fluorochrome measured were calculated using unstained and single fluorochrome-stained cells. For analysis, exclusively the single events were selected on the basis of forward scatter-area versus forward scatter-height. The overall thymocyte profile was studied

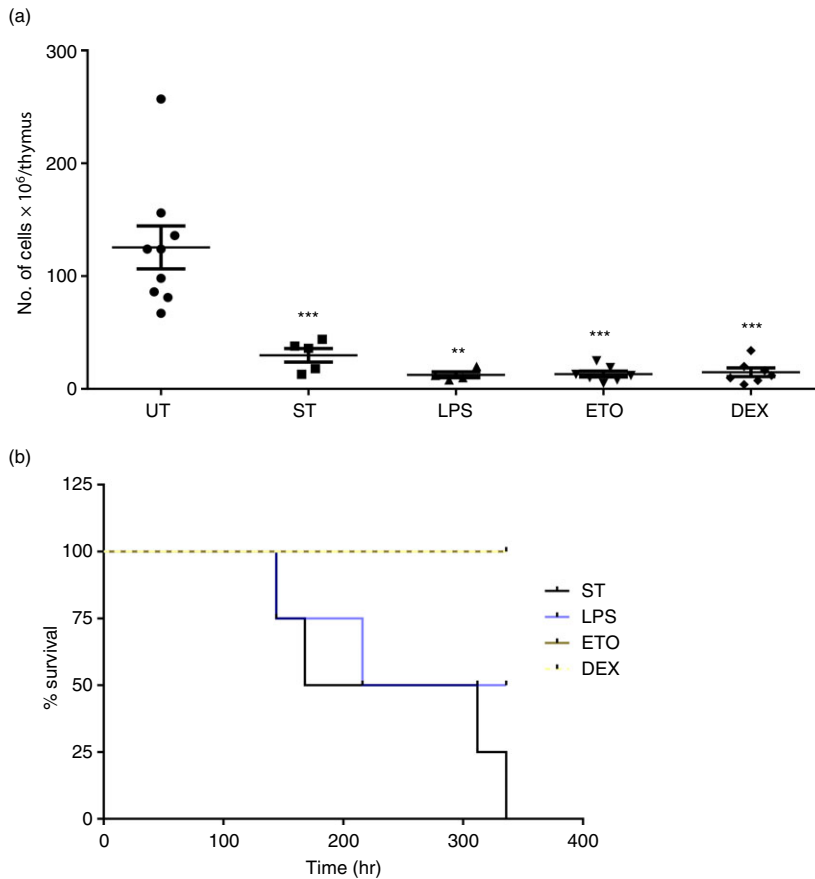


**Figure 1.** Lipopolysaccharide (LPS), etoposide (Eto) and dexamethasone (Dex) induce severe thymic atrophy in BALB/c mice. Six- to 8-week-old male BALB/c mice were either orally infected with  $\sim 10^9$  CFU of *Salmonella* Typhimurium or were intraperitoneally injected with LPS (4 mg/kg), Eto (100 mg/kg) or Dex (15 mg/kg). On day 5 post-infection (ST) and day 4 post-intraperitoneal treatment, the mice, along with the control untreated mice (UT), were killed. (a) The thymi were harvested and the viable cell numbers in the organs were quantified by Trypan blue exclusion assay using a haemocytometer. (b) The mice were monitored at 8-hr intervals for survival after infection or intraperitoneal treatment. The dot plots are depicted as mean  $\pm$  SEM of four to nine mice per group. The two-tailed Mann–Whitney test was used for statistical analysis,  $**P \leq 0.01$ ,  $***P \leq 0.001$  and ns: not significant. The statistical significances denoted on the experimental groups are in comparison with the UT group. The survival curves contained four mice per group.

using the CD4 and CD8 surface markers, and the major thymocyte subsets DN ( $CD4^- CD8^-$ ), DP ( $CD4^+ CD8^+$ ) and SP ( $CD4^+ CD8^-/CD4^- CD8^+$ ) were gated on. Furthermore, to study the DN population, the CD44 and CD25 surface expression profile was investigated. The density plots of CD5 versus CD3 were analysed to quantify the DP thymocyte subset, while CD24 and CD3 plots were used to examine the  $CD4^+$  and  $CD8^+$  SP subsets.

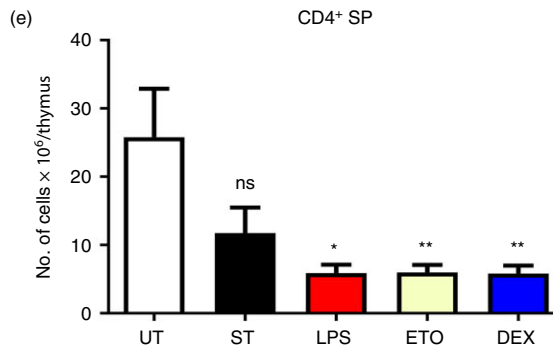
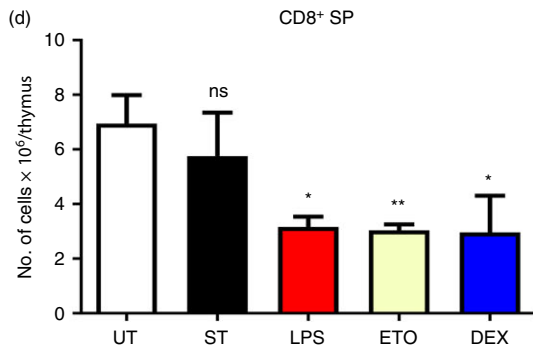
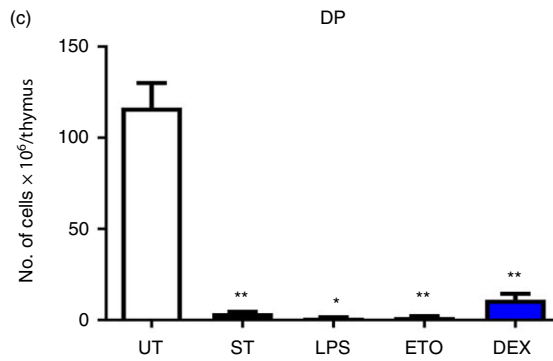
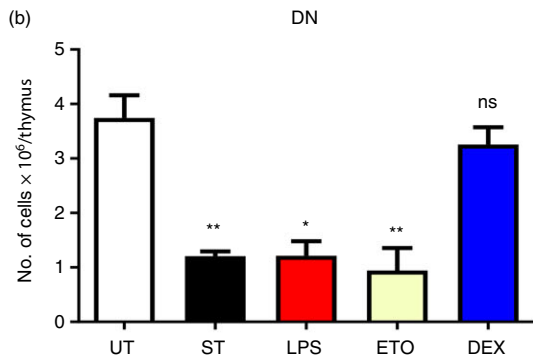
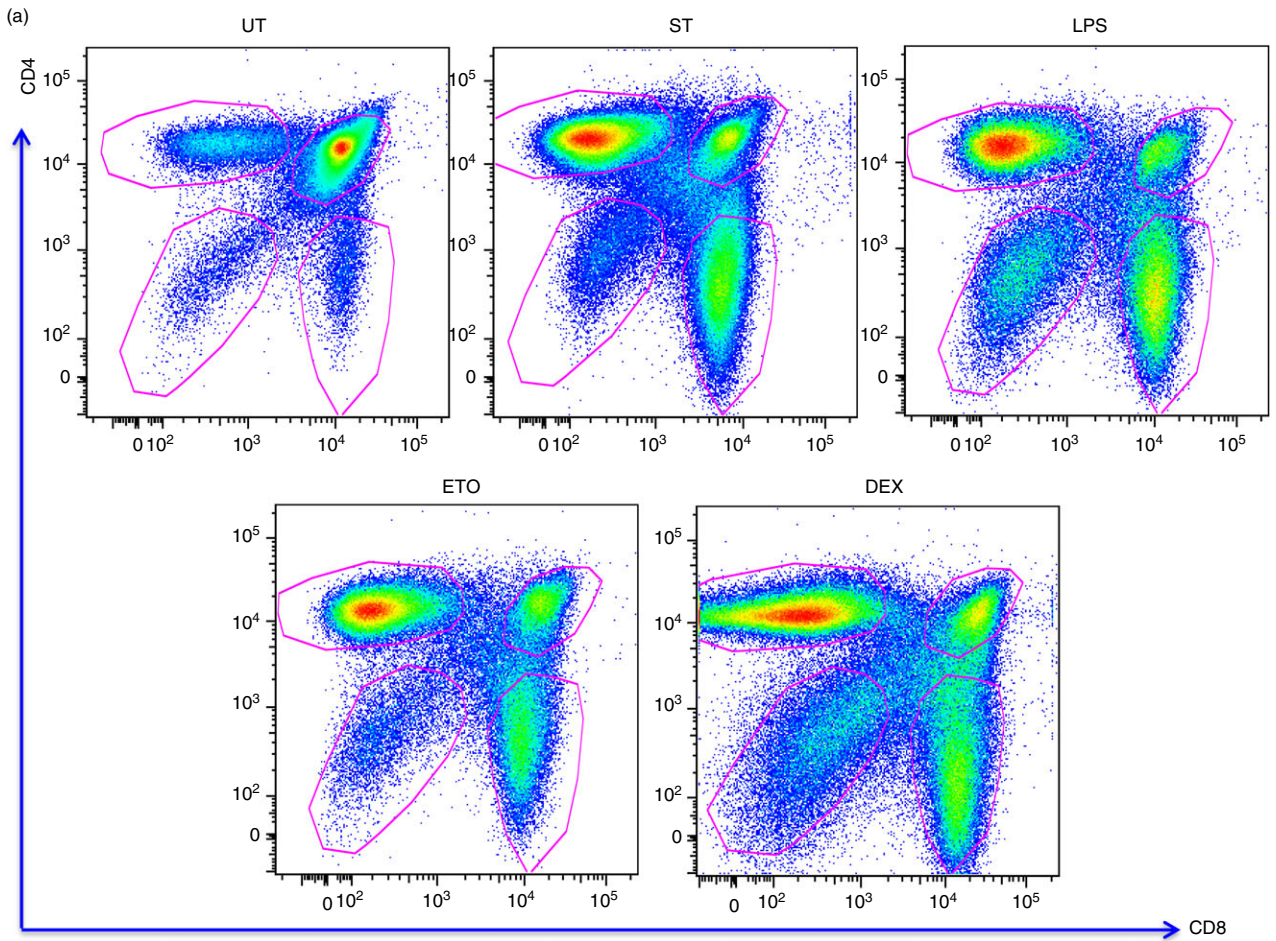
The intracellular ROS amounts were quantified using the DCFDA (2',7'-dichlorofluorescein diacetate, Calbiochem, Burlington, MA) assay. The thymocytes were stained in the dark with  $10 \mu\text{M}$  of DCFDA for 15 min at  $37^\circ$ . Subsequently, the cells were washed with PBS and were acquired on the flow cytometer.<sup>28</sup> The intracellular ROS data are represented as median

fluorescence intensity (MFI) fold change, calculated by obtaining the DCFDA MFI of the samples and dividing the values with the DCFDA MFI of untreated thymocytes values. All FACS data were plotted and analysed using the softwares, FLOWJO (9.9.5) and FACS DIVA (8.0.1).

#### Statistical analysis

Microsoft EXCEL and GRAPHPAD PRISM 5 softwares were used to plot and analyse the data. Statistical significances were calculated using the Mann–Whitney *U*-test or the two-way analysis of variance ( $*P \leq 0.05$ ,  $**P \leq 0.01$ ,  $***P \leq 0.001$ , nd: not detected and ns: not significant). Wherever not indicated, the statistical significances

**Figure 2.** Depletion of different thymocyte subsets occurs across the various modes of thymic atrophy. Male BALB/c mice were either orally infected with *Salmonella* Typhimurium or intraperitoneally administered with lipopolysaccharide (LPS), etoposide (Eto) and dexamethasone (Dex). Along with the control untreated mice (UT), the infected mice (ST) were killed on day 5 post-infection, while the intraperitoneally treated mice were killed on day 4. The thymi were harvested and the thymocytes were stained for cell-surface expression of the T-cell co-receptors, CD4 and CD8. The density plots of CD4 versus CD8 were constructed and (a) the representative density plots are depicted. The number of cells in the major thymocyte subsets, i.e. (b) double-negative (DN) ( $CD4^- CD8^-$ ), (c) double-positive (DP) ( $CD4^+ CD8^+$ ), (d)  $CD8^+$  single-positive (SP) ( $CD4^- CD8^+$ ) and (e)  $CD4^+$  SP ( $CD4^+ CD8^-$ ), was quantified. Data are shown as mean  $\pm$  SEM of four to eight mice per group. Statistical analysis was performed using the two-tailed Mann–Whitney test,  $*P \leq 0.05$ ,  $**P \leq 0.01$  and ns: not significant. The statistical significances denoted on the experimental groups are in comparison with the UT group.



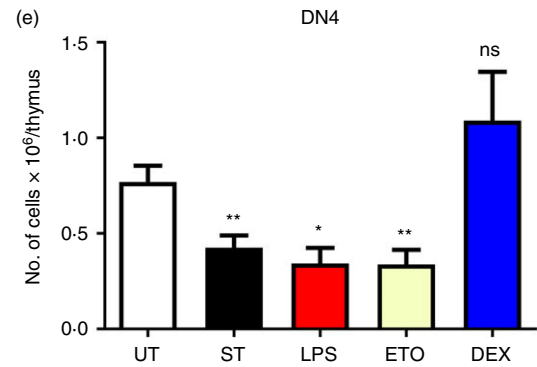
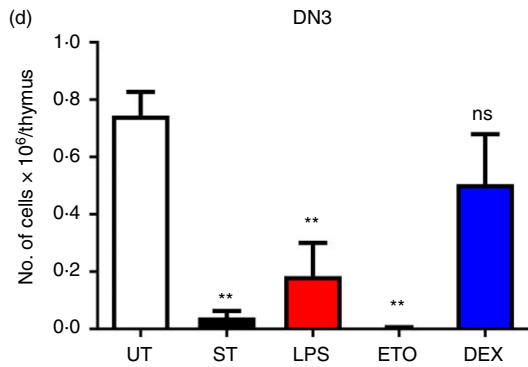
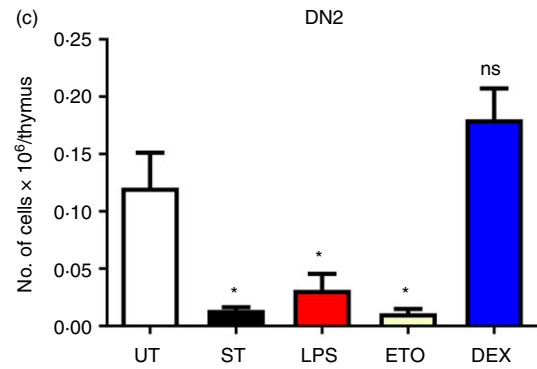
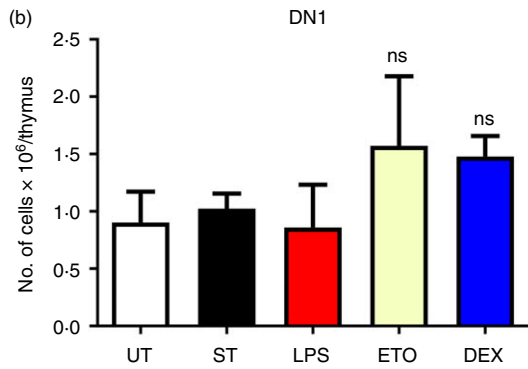
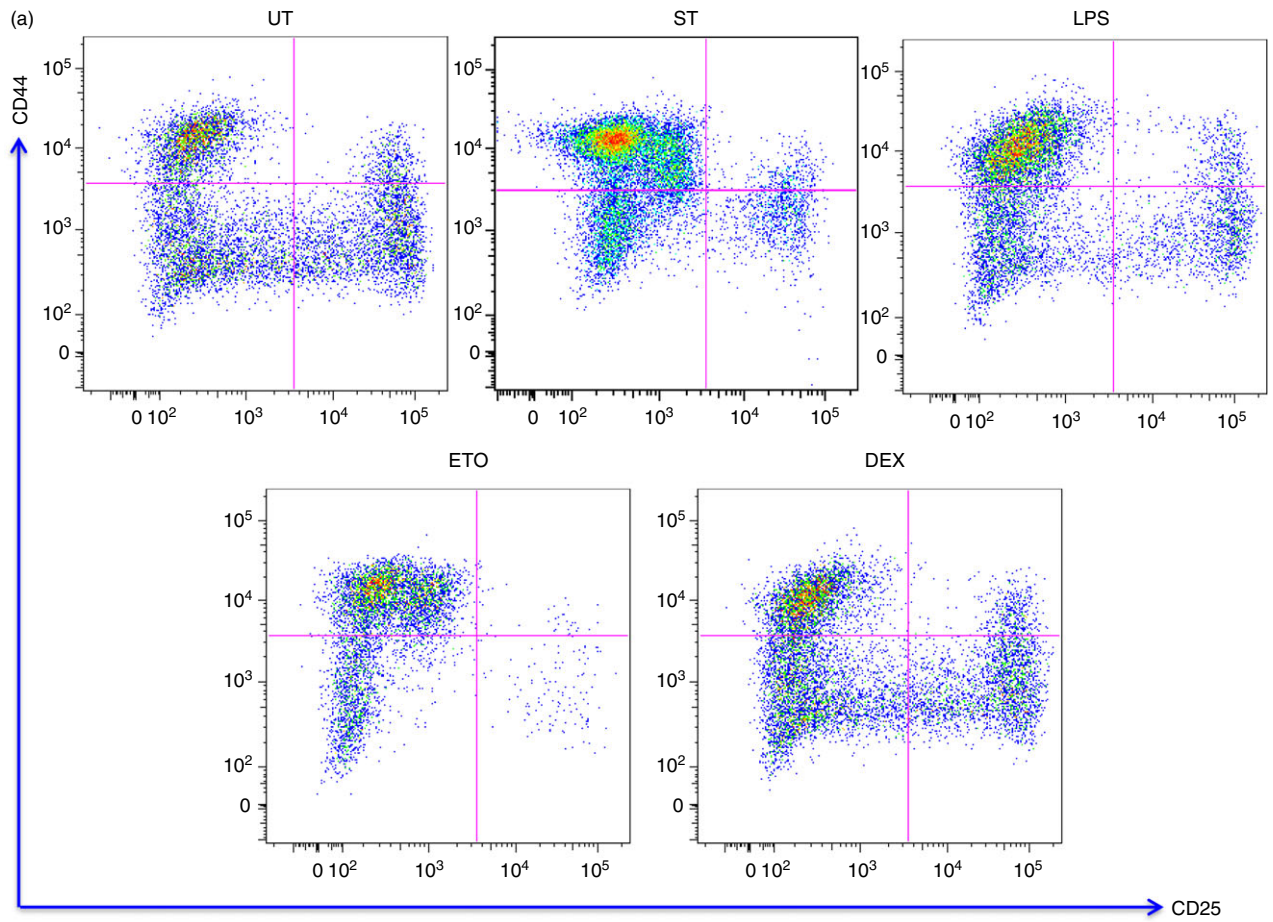


**Figure 3.** *Salmonella* Typhimurium-, lipopolysaccharide (LPS) and etoposide (Eto) -induced thymic atrophy result in the loss of DN2–4 cells. BALB/c mice were either infected with *Salmonella* Typhimurium or treated with LPS, Eto or dexamethasone (Dex). Along with the untreated (UT) mice, the 5-day infected mice (ST) were killed, while the intraperitoneally treated mice were killed on day 4. The thymi were harvested and the thymocytes were stained for cell-surface expression of CD4, CD8, CD44 and CD25 to study the double-negative (DN) ( $CD4^- CD8^-$ ) thymocyte subsets. (a) The density plots of the DN subpopulations were constructed and the representative plots are depicted. The cell numbers were estimated in the (b) DN1 ( $CD4^- CD8^- CD44^+ CD25^-$ ), (c) DN2 ( $CD4^- CD8^- CD44^+ CD25^+$ ), (d) DN3 ( $CD4^- CD8^- CD44^- CD25^+$ ) and (e) DN4 ( $CD4^- CD8^- CD44^- CD25^-$ ) subsets. Data are shown as mean  $\pm$  SEM of four to seven mice per group. Two-tailed Mann–Whitney test was performed to analyse for statistical significance, \* $P \leq 0.05$ , \*\* $P \leq 0.01$  and ns: not significant. The statistical significances denoted on the experimental groups are in comparison with the UT group.

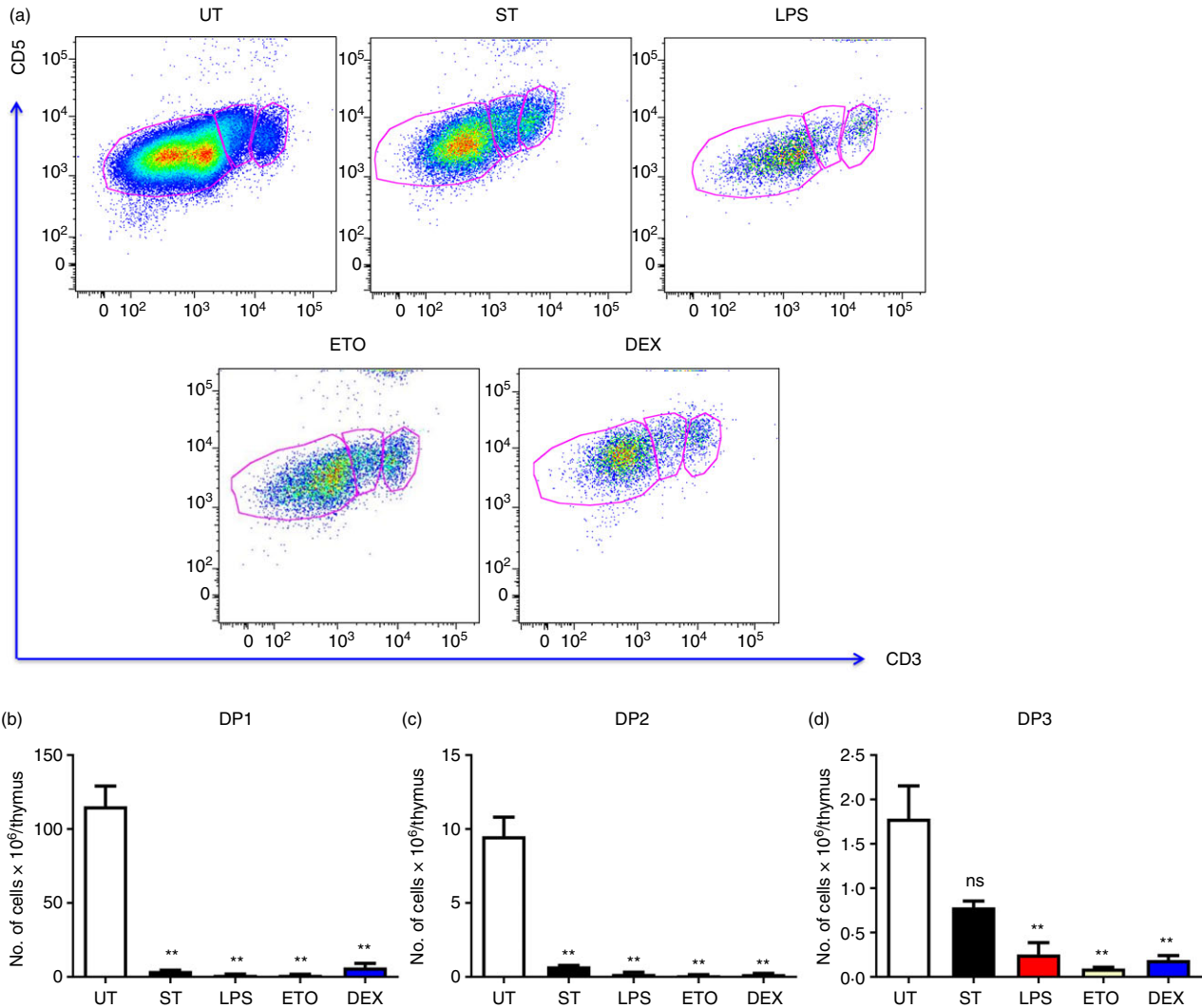


**Figure 4.** Lipopolysaccharide (LPS), etoposide (Eto) and dexamethasone (Dex) -mediated thymic atrophy result in the depletion of DP1–3 thymocytes. The *Salmonella* Typhimurium-infected (ST) mice were killed on day 5 of infection, while the LPS-, Eto- or Dex-treated mice were killed on day 4 of injection. The thymi from these mice as well as from control untreated mice (UT) were harvested and the thymocytes were stained for cell-surface expression of CD4, CD8, CD5 and CD3 to study the double-positive (DP) ( $CD4^+ CD8^+$ ) subset. (a) The density plots of the DP subpopulations were constructed and the representative plots are depicted. The (b) DP1 ( $CD4^+ CD8^+ CD5^{lo} CD3^{lo}$ ), (c) DP2 ( $CD4^+ CD8^+ CD5^{hi} CD3^{int}$ ) and (d) DP3 ( $CD4^+ CD8^+ CD5^{int} CD3^{hi}$ ) cell numbers in the DP compartment were estimated. Data are shown as mean  $\pm$  SEM of four to six mice per group. The two-tailed Mann–Whitney test was used to assess for statistical significance \*\* $P \leq 0.01$  and ns: not significant. The statistical significances denoted on the experimental groups are in comparison with the UT group.

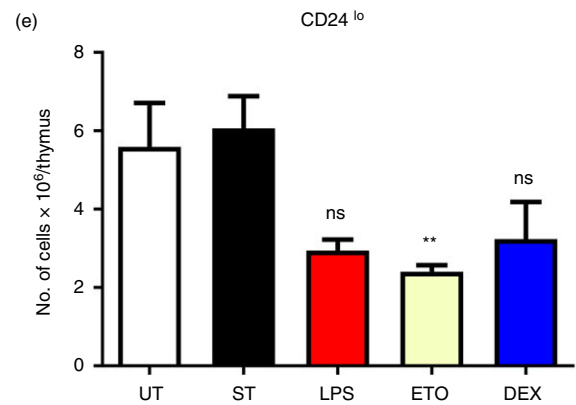
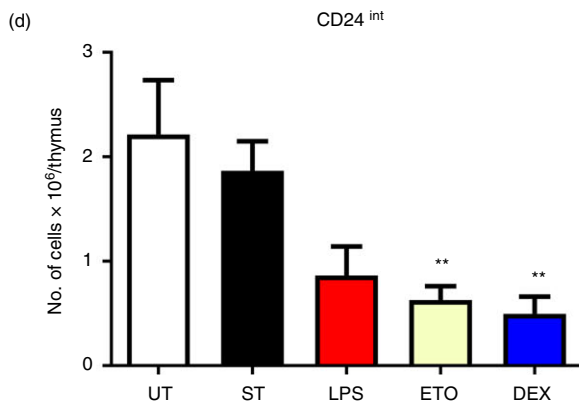
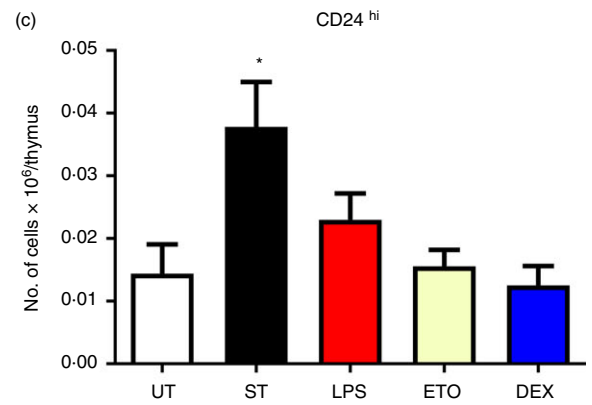
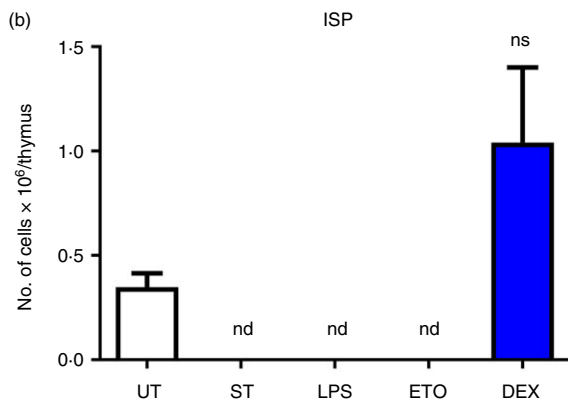
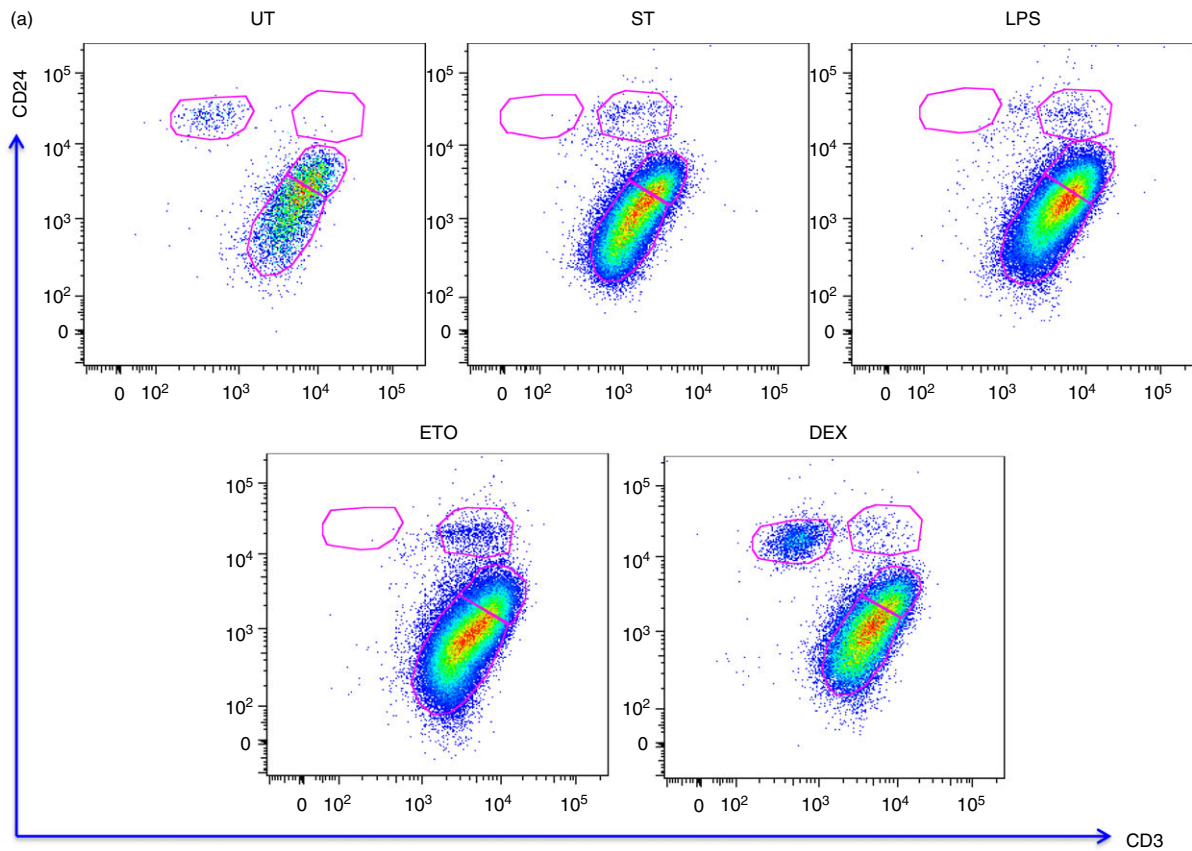




**Figure 5.** Immature single-positive (ISP) thymocytes are completely depleted during *Salmonella* Typhimurium-, etoposide (Eto-) and lipopolysaccharide (LPS) -induced thymic atrophy. Mice were either orally infected with *S. Typhimurium* or intraperitoneally injected with LPS, Eto or dexamethasone (Dex). The mice were killed 5 days post-infection (ST) and 4 days post-intraperitoneal treatment along with the control untreated (UT) mice. The thymi were harvested and the thymocytes were stained for cell-surface expression of CD4, CD8, CD24 and CD3. The CD24 versus CD3 density plots of CD8<sup>+</sup> SP thymocytes were constructed and (a) the representative density plots are shown. The (b) ISP (CD4<sup>-</sup> CD8<sup>+</sup> CD3<sup>lo</sup> CD24<sup>hi</sup>), (c) CD24<sup>hi</sup> (CD4<sup>-</sup> CD8<sup>+</sup> CD3<sup>hi</sup> CD24<sup>hi</sup>), (d) CD24<sup>int</sup> (CD4<sup>-</sup> CD8<sup>+</sup> CD3<sup>hi</sup> CD24<sup>int</sup>) and (e) CD24<sup>lo</sup> (CD4<sup>-</sup> CD8<sup>+</sup> CD3<sup>hi</sup> CD24<sup>lo</sup>) cells in the CD8<sup>+</sup> SP compartment were quantified. Data are depicted as mean ± SEM of four to eight mice per group. The two-tailed Mann–Whitney test was used to analyse for statistical significance, \**P* ≤ 0.05, \*\**P* ≤ 0.01, nd: not detected and ns: not significant. The statistical significances denoted on the experimental groups are in comparison with the UT group.

denoted on the experimental groups are in comparison with the control untreated (UT) group/s.

## Results

### *Salmonella* Typhimurium infection and LPS, Eto and Dex treatment induce thymic atrophy

Preliminary experiments were performed to ascertain the optimum amounts of LPS, Eto and Dex required to induce thymic atrophy comparable to the levels induced by oral *S. Typhimurium* infection in BALB/c mice. *Salmonella* Typhimurium infection-induced thymic atrophy; the system of thymic atrophy well established in our laboratory<sup>5,23,28</sup> was considered as the positive control. The mice were either orally infected with ~10<sup>9</sup> CFU of *S. Typhimurium* or intraperitoneally injected with the mentioned doses of LPS, Eto or Dex. After 5 days of infection and on day 4 of intraperitoneal treatment, the mice were killed and the cellularity of the thymi was determined. Infection led to a five- to sixfold reduction in the thymic cellularity. Severe thymic atrophy was observed in mice treated with the mentioned doses of LPS, Eto and Dex after day 4 of treatment. LPS and Dex displayed enhanced potency, compared with Eto, as they induced similar extents of thymic atrophy at lower concentrations (Fig. 1a). The increased susceptibility of thymocytes towards Dex was in accordance with *in vitro* experiments. Dex at a dose of 1 ng/ml depleted thymocytes *in vitro*, whereas LPS and Eto induced significant cell death in µg/ml amounts. On the other hand, *S. Typhimurium* was unable to deplete thymocytes *in vitro*<sup>23</sup> (see Supplementary material, Fig. S1). Subsequently, the *S. Typhimurium*-infected mice and the mice given the optimum doses of the compounds were monitored at 8-hr intervals for survival. *Salmonella* Typhimurium resulted in 100% mortality by 14 days of infection, whereas 50% of mice survived LPS treatment. Eto and Dex treatment did not lead to the death of mice (Fig. 1b).

### The thymocyte subsets are selectively modulated during the different modes of thymic atrophy

Having standardized the optimum doses of the compounds that induce thymic atrophy, we studied the four major thymocyte subsets – DN, DP, CD8<sup>+</sup> SP and CD4<sup>+</sup>

SP – on the basis of cell-surface CD4 and CD8 expression. *Salmonella* Typhimurium infection depleted the immature thymocyte subsets, DNs and DPs, whereas LPS and Eto treatment reduced all the four thymocyte subsets to varying degrees. On the other hand, Dex specifically reduced the DP, CD8<sup>+</sup> SP and CD4<sup>+</sup> SP cells (Fig. 2). Therefore, different thymocyte subsets displayed varying extents of susceptibility towards the tested treatments.

### DN2–4 thymocytes are depleted during infection, and LPS and Eto treatment

Next, we studied the thymocyte subpopulations in detail, starting with the DN cells. The thymocytes were stained for surface expression of CD4, CD8, CD44 and CD25. The CD4<sup>-</sup> CD8<sup>-</sup> thymocytes were gated, and the CD44 versus CD25 density plots were constructed to study the DN thymocyte subsets. DN2–4 cells were depleted during infection-induced thymic atrophy, whereas the DN1 cells remained unchanged. Similar manifestations were also observed in mice treated with LPS or Eto. Contrastingly, Dex treatment did not significantly alter the cellularity of the DN subsets (Fig. 3).

### DP1–3 thymocytes are reduced during LPS-, Eto- and Dex-mediated thymic atrophy

Subsequently, we studied the DP subsets by gating on the CD4<sup>+</sup> CD8<sup>+</sup> cells and by analysing the cells on the basis of CD5 and CD3 expression. *Salmonella* Typhimurium infection reduced the DP1 and DP2 cells, but not the DP3 cells (Fig. 4).<sup>5</sup> On the other hand, the DP1–3 cells were significantly depleted in mice treated with LPS, Eto and Dex on day 4 (Fig. 4).

### Infection, LPS and Eto completely deplete the ISP cells post-thymic atrophy

The CD8<sup>+</sup> SP compartment was analysed by studying the expression of CD24 and CD3 (Fig. 5). Thymic atrophy induced by *S. Typhimurium* infection and treatments with LPS and Eto completely depleted the CD4<sup>-</sup> CD8<sup>+</sup> CD3<sup>lo</sup> CD24<sup>hi</sup> ISP cells on day 4. Surprisingly, Dex had no significant effect on these cells despite the fact that ISP cells are reported to be cortisol sensitive.<sup>29</sup> A significant

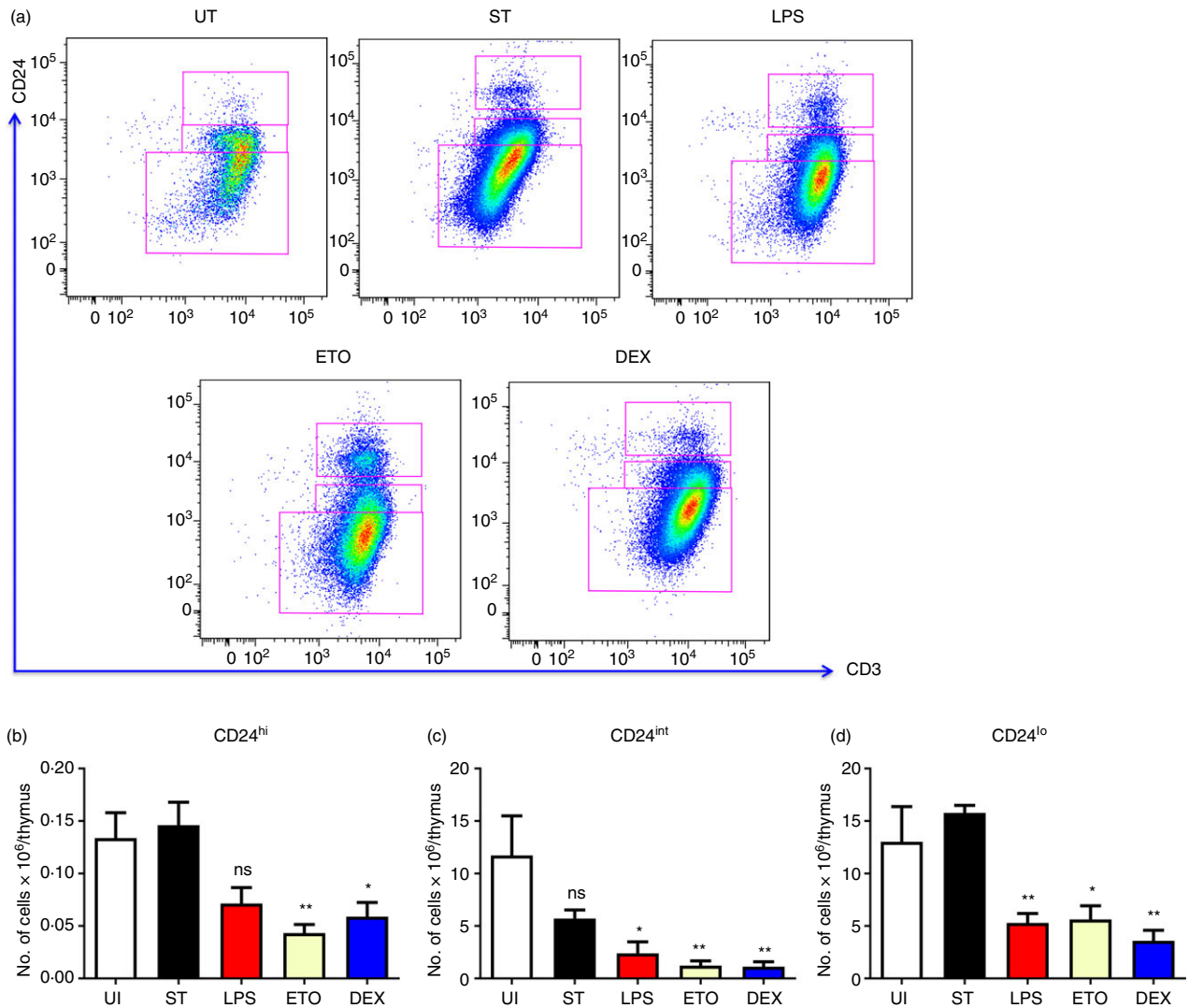


**Figure 6.** Thymic atrophy induced by lipopolysaccharide (LPS), etoposide (Eto) and dexamethasone (Dex) treatment led to loss of CD4<sup>+</sup> single-positive (SP) cells. The orally infected (ST) mice were killed on day 5, while the intraperitoneally treated BALB/c mice along with the control untreated (UT) mice were killed on day 4. The thymi were harvested and the thymocytes were stained for cell-surface expression of CD4, CD8, CD24 and CD3. CD24 versus CD3 density plots of the CD4<sup>+</sup> SP thymocytes were constructed and (a) the representative plots are depicted. The (b) CD24<sup>hi</sup> (CD4<sup>+</sup> CD8<sup>-</sup> CD3<sup>hi</sup> CD24<sup>hi</sup>), (c) CD24<sup>int</sup> (CD4<sup>+</sup> CD8<sup>-</sup> CD3<sup>hi</sup> CD24<sup>int</sup>) and the (d) CD24<sup>lo</sup> (CD4<sup>+</sup> CD8<sup>-</sup> CD3<sup>hi</sup> CD24<sup>lo</sup>) cells in the CD4<sup>+</sup> SP compartment were quantified. Data are shown as mean ± SEM of seven or eight mice per group. The two-tailed Mann–Whitney test was used for analysing statistical significance, \**P* ≤ 0.05, \*\**P* ≤ 0.01 and ns: not significant. The statistical significances denoted on the experimental groups are in comparison with the UT group.

accumulation of the less mature CD24<sup>hi</sup> cells was observed after infection-induced thymic atrophy<sup>5</sup> but was not found in the other modes of thymic atrophy. Eto and Dex by day 4 reduced the cellularity of the CD24<sup>int</sup> cells whereas Eto also reduced the numbers of CD24<sup>lo</sup> cells (Fig. 5).

#### CD4<sup>+</sup> SP cells are reduced during LPS, Eto and Dex treatment

Similar to the CD8<sup>+</sup> SP compartment, the CD4<sup>+</sup> SP compartment was analysed (Fig. 6). LPS, Eto and Dex treatment resulted in loss of the CD24<sup>int-lo</sup> cells in the CD4<sup>+</sup> SP

compartment on day 4 whereas not much change was observed during infection (Fig. 6). In addition, Eto and Dex treatment depleted CD24<sup>hi</sup> cells. The changes observed in the thymocyte subpopulations during different modes of thymic atrophy are summarized in Table 1.

#### ROS mediate thymocyte loss during *S. Typhimurium*- and LPS-induced thymic atrophy in mice

Increased ROS observed in thymocytes<sup>30</sup> often leading to apoptosis, and its inhibition has been shown to rescue thymic atrophy induced by various conditions.<sup>30–33</sup> To

**Table 1.** Summary of changes occurring in the thymocyte subpopulations in the models of thymic atrophy studied

	ST		LPS		ETO	DEX
	- NAC	+ NAC	- NAC	+ NAC		
DN1 (CD4 <sup>-</sup> CD8 <sup>-</sup> CD44 <sup>+</sup> CD25 <sup>-</sup> )	NE	NE	NE	NE	NE	NE
DN2 (CD4 <sup>-</sup> CD8 <sup>-</sup> CD44 <sup>+</sup> CD25 <sup>+</sup> )	↓	↑	↓	↑	↓	NE
DN3 (CD4 <sup>-</sup> CD8 <sup>-</sup> CD44 <sup>-</sup> CD25 <sup>+</sup> )	↓	↑	↓	↑	↓	NE
DN4 (CD4 <sup>-</sup> CD8 <sup>-</sup> CD44 <sup>-</sup> CD25 <sup>-</sup> )	↓	↓	↓	↑	↓	NE
ISP (CD4 <sup>-</sup> CD8 <sup>+</sup> CD3 <sup>lo</sup> CD24 <sup>hi</sup> )	↓	↑	↓	↑	↓	NE
DP1 (CD4 <sup>+</sup> CD8 <sup>+</sup> CD5 <sup>lo</sup> CD3 <sup>lo</sup> )	↓	↑	↓	↑	↓	↓
DP2 (CD4 <sup>+</sup> CD8 <sup>+</sup> CD5 <sup>hi</sup> CD3 <sup>int</sup> )	↓	↑	↓	↑	↓	↓
DP3 (CD4 <sup>+</sup> CD8 <sup>+</sup> CD5 <sup>int</sup> CD3 <sup>hi</sup> )	NE	NE	↓	↑	↓	↓
CD4 <sup>-</sup> CD8 <sup>+</sup> CD3 <sup>hi</sup> CD24 <sup>hi</sup>	↑	↑	NE	NE	NE	NE
CD4 <sup>-</sup> CD8 <sup>+</sup> CD3 <sup>hi</sup> CD24 <sup>int</sup>	NE	NE	NE	NE	↓	↓
CD4 <sup>-</sup> CD8 <sup>+</sup> CD3 <sup>hi</sup> CD24 <sup>lo</sup>	NE	NE	NE	NE	↓	NE
CD4 <sup>+</sup> CD8 <sup>-</sup> CD3 <sup>hi</sup> CD24 <sup>hi</sup>	NE	NE	NE	NE	↓	↓
CD4 <sup>+</sup> CD8 <sup>-</sup> CD3 <sup>hi</sup> CD24 <sup>int</sup>	NE	NE	↓	↑	↓	↓
CD4 <sup>+</sup> CD8 <sup>-</sup> CD3 <sup>hi</sup> CD24 <sup>lo</sup>	NE	NE	↓	NE	↓	↓

Dex, dexamethasone; DN, double-negative; DP, double-positive; Eto, etoposide; LPS, lipopolysaccharide; ST, *Salmonella* Typhimurium.

The downward arrows indicate depletion in cellularity, the upward arrows show populations with increased cellularity, NE denotes no effect, and the red circles indicate the populations that were rescued by *N*-acetyl cysteine (NAC) administration.

study the roles of ROS during the various models of thymic atrophy, we used the ROS quencher, NAC. The thymocytes from control, infected and treated mice were stained with DCFDA to detect intracellular ROS. The total ROS amounts in the thymocytes increased during *S. Typhimurium*- and LPS-induced thymic atrophy and NAC treatment led to its reduction. Contrastingly, ROS induction was absent in thymocytes from Eto- and Dex-treated mice (Fig. 7a). Upon NAC treatment, reduction in the extent of thymic atrophy during *S. Typhimurium* infection and LPS treatment was observed. However, NAC provision failed to reduce the thymic atrophy in Eto- and Dex-treated mice (Fig. 7b).

#### Cortisol, but not the pro-inflammatory cytokines, in sera is lowered upon NAC administration during infection

The degree of thymic atrophy directly correlates with the amount of *S. Typhimurium* infection load.<sup>5,23</sup> Therefore, we investigated the effect of NAC treatment on the bacterial infection load in the liver, spleen and Peyer's patches. NAC did not have any significant effect on the bacterial burden (Fig. 8). Numerous studies indicate the occurrence of thymic atrophy as a direct consequence of inflammatory

processes, involving TNF- $\alpha$ ,<sup>24,25,34</sup> IL-6,<sup>11,34</sup> IFN- $\gamma$ ,<sup>5,23,35-38</sup> and GCs.<sup>5,19-23,36,39</sup> Therefore, we investigated whether NAC exerted its thymopoietic effects by dampening inflammatory responses. LPS did not show any up-regulation of the cytokines on day 4 post-treatment. However, significant induction in levels of TNF- $\alpha$ , IL-6 and IFN- $\gamma$  could be observed only during *S. Typhimurium* infection. Importantly, the levels of these cytokines remained unchanged after NAC treatment in *S. Typhimurium*-infected mice (Fig. 9a-c). However, the cortisol amounts in sera of the infected mice were significantly reduced after NAC administration, suggesting that the thymopoietic property displayed by NAC may, at least in part, be due to reduction in cortisol amounts (Fig. 9d).

#### NAC rescues the depletion of the DN, ISP and the DP thymocytes during *S. Typhimurium*- and LPS-mediated thymic atrophy

Next, we investigated the effects of NAC administration on the thymocyte subpopulations in infected and LPS-treated mice. The depletion of the DN and the DP thymocytes, but not SPs, in the infected and LPS-treated mice was rescued after NAC treatment (see Supplementary material, Fig. S2). The decrease in the cellularity of the DN2-3 post-infection

and DN2–4 post-LPS treatment was rescued by NAC administration, while the DN1 cells remained unaffected (see Supplementary material, Fig. S3a–d). In the DP subset, NAC treatment reduced the depletion of the DP1 and DP2 cells during infection and LPS treatment. The decrease of DP3 cells in LPS-treated mice was also rescued to a significant extent upon NAC supplementation (see Supplementary material, Fig. S3e–g). The ISP cells in the CD8<sup>+</sup> SP compartment are the most sensitive thymocyte subpopulation to depletion during *S. Typhimurium*-induced thymic atrophy.<sup>5</sup> The complete depletion of the ISPs during infection and LPS treatment was rescued to a full extent post-NAC administration. In contrast, the accumulation of the less mature CD24<sup>hi</sup> CD8<sup>+</sup> SP cells, observed during infection-induced thymic atrophy, was not lowered by NAC treatment (see Supplementary material, Fig. S4a). NAC also did not exert any effects on the CD24<sup>hi</sup> cells in the CD4<sup>+</sup> SP compartment (see Supplementary material, Fig. S4e). The comparatively more mature CD24<sup>int-lo</sup> cells in both the SP compartments remained largely unchanged upon NAC treatment in the thymi of the infected mice. However, in LPS-treated mice, NAC was successful in rescuing the loss of CD24<sup>int</sup> cells in the CD4<sup>+</sup> SP compartment (see Supplementary material, Fig. S4f). The effects of NAC on the thymocyte subpopulations during infection and LPS treatment are tabulated in Table 1.

## Discussion

The comparative study of thymic subpopulations that are affected during various modes of thymic atrophy

constitutes a neglected area of research. Here, we have used multicolour flow cytometry<sup>5</sup> to study in detail the thymocyte subpopulations in various important models of thymic atrophy. Comparative studies of the thymocyte subpopulations revealed distinct changes occurring across the various models of thymic atrophy which are summarized in Table 1 and Fig. 10. The DN cells might be reduced during thymic atrophy as a result of loss in supply of early thymic progenitors from the bone marrow, block in the developmental pathway at a specific DN stage or apoptosis of the DN cells. In the models of thymic atrophy studied here, the third scenario is more likely. Depletion of the DN2–4 thymocytes occurs during *S. Typhimurium* infection-induced thymic atrophy in C57BL/6 mice, with the cellularity of DN1 cells being unaffected.<sup>5</sup> Similar results were obtained in infected BALB/c mice and BALB/c mice treated with LPS and ETO (Fig. 3). Reduction of early thymic progenitors or a block at a specific developmental stage would manifest in depletion of the DN1 cells or increase in cellularity of a specific DN cell subset, respectively, neither of which was observed. Interestingly, such observations are also found upon administration of TNF- $\alpha$ .<sup>40</sup> In addition, in aged mice, the lack of expression of the T-cell-specific transcription factor, TCF-1 results in a developmental block at the DN1 stage.<sup>41</sup> In case of Eto-mediated DN2–4 loss, the results are in accordance with previous reports stating that the chemotherapeutic drug targets proliferating cells.<sup>14,42</sup> DN1 cells reside for ~10 days before progressing into the DN2 stage.<sup>43</sup> Depletion of DN1 cells during regular Eto treatment over longer periods of time cannot be

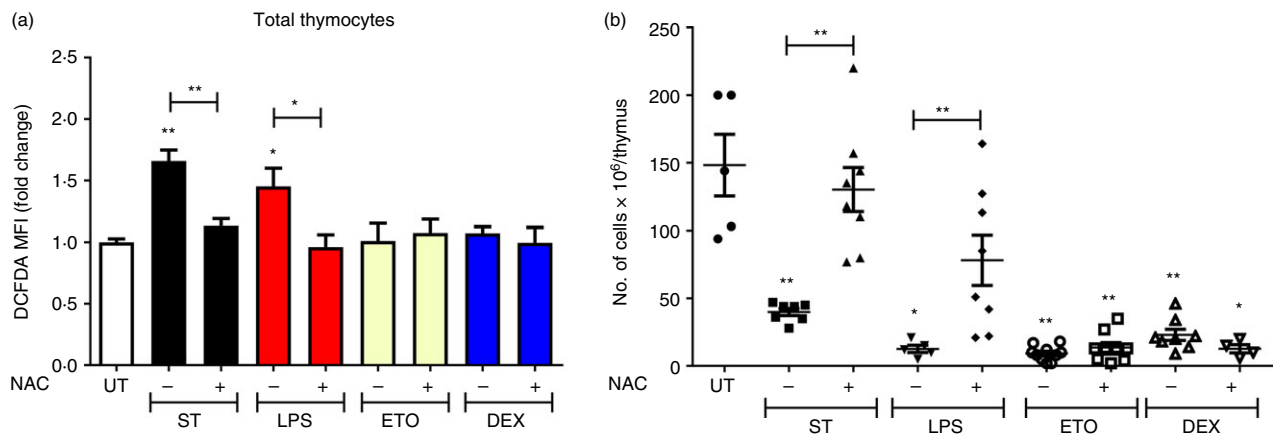


**Figure 7.** Infection- and lipopolysaccharide (LPS)-induced thymic atrophy are reactive oxygen species (ROS)-dependent. BALB/c mice were either orally infected with *Salmonella Typhimurium* or intraperitoneally treated with LPS, etoposide (Eto) or dexamethasone (Dex). After 16 and 32 hr, the mice were provided with either phosphate-buffered saline (– NAC) or 100 mg/kg *N*-acetyl cysteine (+ NAC) by oral gavage. On days 4 and 5 after intraperitoneal treatment or infection (ST), respectively, the mice were killed along with the control UT mice. The thymi were harvested and the thymocytes were stained with 2',7'-dichlorofluorescein diacetate (DCFDA) and its (a) median fluorescence intensity (MFI) fold change in total thymocytes was calculated. The total number of viable (b) thymocytes was quantified by Trypan blue exclusion assay using a haemocytometer. Data are shown as mean  $\pm$  SEM of four to ten mice per group. The two-tailed Mann–Whitney test was used to analyse for statistical significance among the experimental groups, \* $P \leq 0.05$ , \*\* $P \leq 0.01$  and ns: not significant. The statistical significances denoted on the experimental groups are in comparison with the UT group.

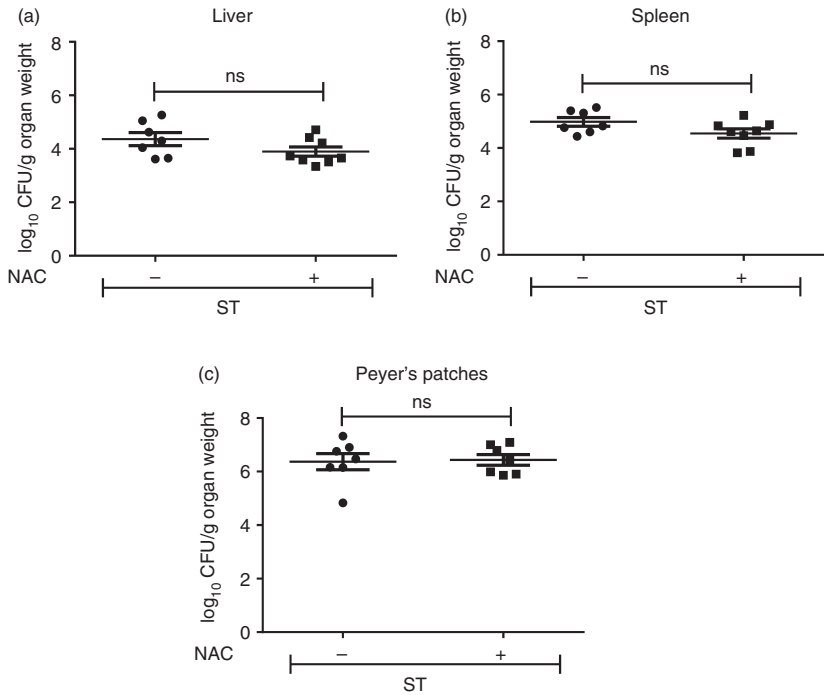


**Figure 8.** *N*-Acetyl cysteine (NAC) treatment does not modulate *Salmonella* Typhimurium infection burden. BALB/c mice were orally infected with  $\sim 10^9$  CFU of *S. Typhimurium*/mouse. After 16 and 32 hr, the mice were provided with either phosphate-buffered saline (–NAC) or NAC (+NAC) by oral gavage. On day 5 post-infection, the mice were killed and the organs were harvested. The bacterial load in (a) liver, (b) spleen and (c) Peyer's patches was estimated. Data are shown as mean  $\pm$  SEM of eight mice per group and the statistical significance was assessed by the two-tailed Mann–Whitney test, ns: not significant.

discounted. Dex alone did not particularly affect the cellularity of the DN cells, which is in agreement with another study.<sup>44</sup> Although GCs are known to play a role in lowering the survival of DNs during infection,<sup>5</sup> most likely, the combination of GCs along with other host factors induced with infection may be involved.

*Salmonella* Typhimurium infection in BALB/c mice resulted in loss of the DP1 and DP2 cells, while the DP3 cells were comparatively more resistant, which is similar in C57BL/6 mice.<sup>5</sup> Administration of LPS in mice leads to a rapid up-regulation of pro-inflammatory cytokines and their levels wane at later time-points.<sup>45</sup> Notably, the LPS and infection models differ fundamentally in the kinetics of induction of pro-inflammatory cytokines: induction occurs rapidly with LPS, whereas it is gradual with infection, concomitant with increase in numbers of bacteria.<sup>5,23</sup> This may account for the lack of DP3 accumulation in LPS-treated mice (Figs 4 and 9a–c). During Eto-induced thymic atrophy, the apoptosis of the proliferating cells in the DN and DP subsets<sup>14,42</sup> may contribute towards the depletion of these subsets.

The expression of the GC receptor is highest in DN thymocytes, followed by the CD8<sup>+</sup> SP cells, CD4<sup>+</sup> SP cells and then the DP cells.<sup>44</sup> In spite of low expression of the GC receptor in the DP cells, they display the most sensitivity among the thymocyte subpopulations studied, possibly because of increased amounts of the apoptosis-related protein, dexamethasone-induced gene 2 and low amounts of the anti-apoptotic protein, Bcl2.<sup>46</sup> During *in vivo* Dex treatment, DP cells are significantly depleted and the majority of the surviving DP cells are CD69<sup>+</sup>. It

has been speculated that the DP thymocytes undergoing positive selection are more resistant to Dex-induced apoptosis.<sup>44</sup> Similar results were observed in another study where the T-cell receptor  $\beta$  intermediate (TCR $\beta^{\text{int}}$ ) DP cells were comparatively more resistant to depletion than the TCR- $\beta^{\text{lo}}$  DP cells.<sup>29</sup>

The ISP cells are the earliest thymocyte subset to be depleted during *S. Typhimurium* infection.<sup>5</sup> In this study, the ISPs were completely depleted across the different modes of thymic atrophy except in Dex-treated mice (Fig. 5). LPS is known to rapidly induce GCs<sup>47</sup> and IFN- $\gamma$ ,<sup>45</sup> which may be involved in this observation. In case of Eto, the ISPs were a major target for depletion, as these cells are known to be rapidly proliferating.<sup>48</sup> ISP cells are reported to be sensitive to Dex-induced apoptosis.<sup>29</sup> It should be noted that the effects of Dex on ISPs has been either studied after 8 hr<sup>29</sup> or 48 hr of exposure,<sup>48,49</sup> *in vivo*. However in our study, ISP cells, like DNs, were resistant to Dex treatment (Fig. 5a,b) and our data show that Dex does not reduce the numbers of immature early-stage thymic cells, i.e. DNs and ISPs.

During *S. Typhimurium*-induced thymic atrophy in C57BL/6 mice, CD4<sup>+</sup> SP cells are affected to a lesser extent, whereas CD8<sup>+</sup> SPs are resistant. Also, there is a delay in the differentiation process of SPs and CD24<sup>hi</sup> SPs accumulate in both CD4<sup>+</sup> and CD8<sup>+</sup> SP compartments, which is primarily dependent on infection-induced IFN- $\gamma$ .<sup>5</sup> However, BALB/c mice are less inflammatory compared with C57BL/6 mice,<sup>50,51</sup> display reduced thymic atrophy and mice survival on a comparative basis. It is likely that the lower accumulation of CD24<sup>hi</sup> SPs may be

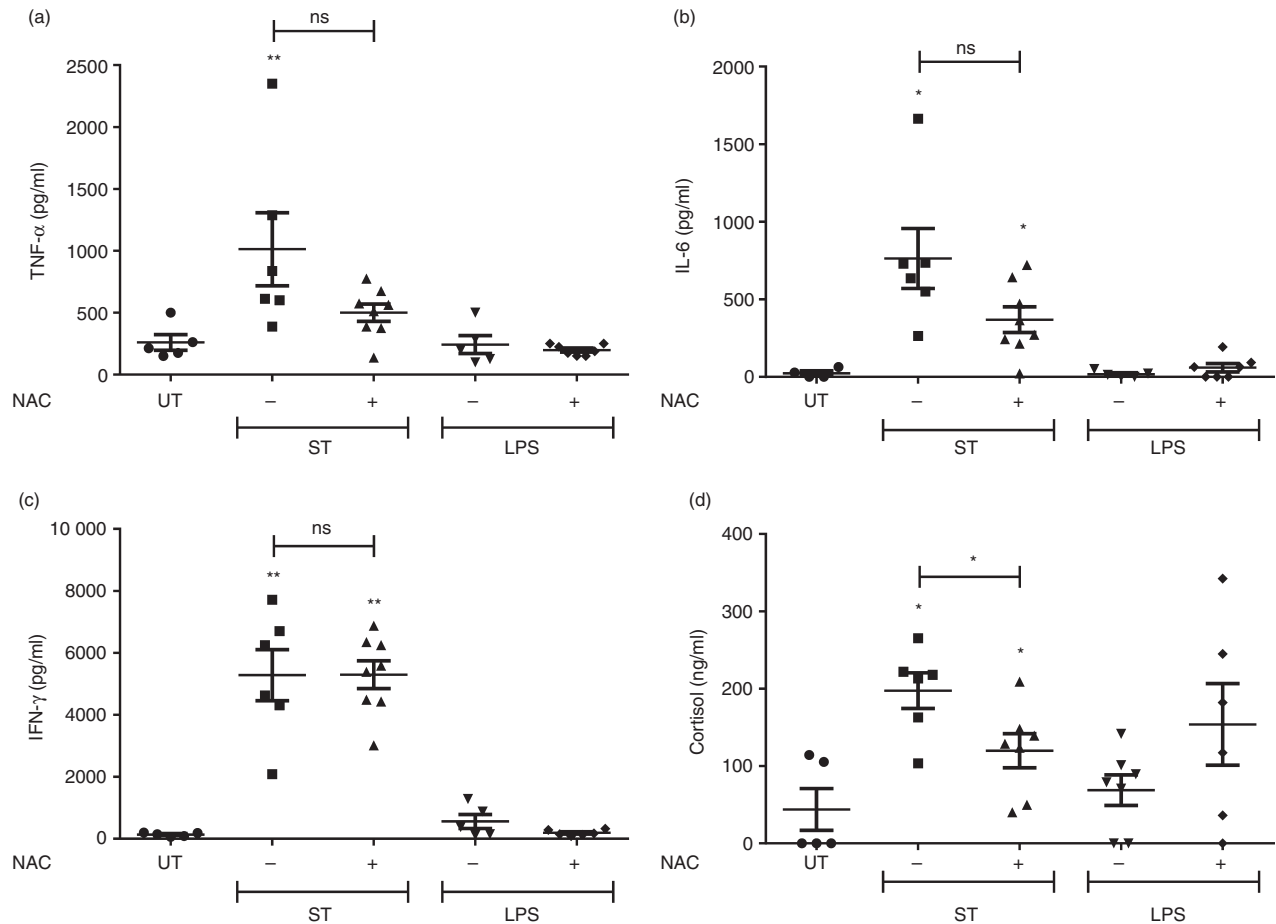


**Figure 9.** N-Acetyl cysteine (NAC) treatment reduces the serum glucocorticoid (GC) amounts in infected mice. BALB/c mice were either infected with *Salmonella* Typhimurium or intraperitoneally injected with lipopolysaccharide (LPS). After 16 and 32 hr, the mice were provided with either phosphate-buffered saline (– NAC) or NAC (+ NAC) by oral gavage. On days 4–5 after infection or treatment, the mice were killed and blood was collected by cardiac puncture. The (a) tumour necrosis factor- $\alpha$  (TNF- $\alpha$ ), (b) interleukin-6 (IL-6), (c) interferon- $\gamma$  (IFN- $\gamma$ ) and (d) cortisol amounts in the sera were quantified by ELISA. Data are shown as mean  $\pm$  SEM of five to eight mice per group. The statistical significance among the experimental groups was calculated by the two-tailed Mann–Whitney test, \* $P \leq 0.05$ , \*\* $P \leq 0.01$  and ns: not significant. The statistical significances denoted on the experimental groups are in comparison with the UT group.

due to the comparatively reduced amounts of infection-induced IFN- $\gamma$  produced in BALB/c mice. Note that there are no major distinctions in the cortisol amounts between C57BL/6 and BALB/c mice<sup>23</sup> (Fig. 9d). Clearly, there are some differences in infection-induced thymic atrophy in the two mouse strains, C57BL/6 and BALB/c, which are tabulated in the Supplementary material (Table S1). LPS did not show any effects on CD8<sup>+</sup> SP cells, whereas CD4<sup>+</sup> SP were lowered. Both Eto and Dex reduced the number of SP thymocytes. The depletion of CD8<sup>+</sup> SPs was the least (Figs 5 and 6), which is in accordance with the estimated proliferation rates of the CD4<sup>+</sup> and CD8<sup>+</sup> SP cells, namely, 46.3% and 27%, respectively.<sup>52</sup>

Thymic atrophy can result due to the direct effects of pathogens (e.g. HIV on CD4<sup>+</sup> T cells) or compounds. Alternatively, it can be due to the induction of host factors, e.g. hormones, cytokines, signalling proteins, ROS, etc., during infection or inflammatory conditions.<sup>6,7</sup> *In vitro*

studies clearly demonstrated that Eto and Dex, at low concentrations, directly lowered the survival of thymocytes (see Supplementary material, Fig. S1), whereas the effects during infection<sup>5,23</sup> or LPS<sup>7</sup> were most likely due to host-induced factors. One of the host-induced factors is the generation of ROS. The involvement of ROS in thymic atrophy is well documented and the supplementation of ROS quenchers or inhibitors is successful in reducing the extent of atrophy during ageing,<sup>31,33</sup> viral infection<sup>32</sup> and tumour growth<sup>30</sup> in mice. Antioxidants such as NAC and vitamin C have been successful in increasing the survival and numbers of CD4<sup>+</sup> T cells in the periphery of HIV patients. In addition, vitamin C has also resulted in the reduction of HIV RNA plasma levels and greater lymphocyte proliferation.<sup>53</sup> However, the direct roles of ROS in thymic atrophy during bacterial infections and LPS treatment and its effects on the distinct subpopulations have not been studied hitherto. Copper chelators inhibit Eto- as well as Dex-induced

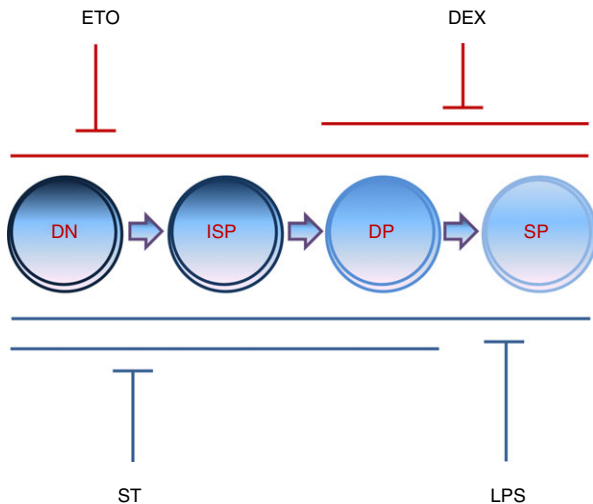


**Figure 10.** The thymocyte subpopulations are selectively depleted during different modes of thymic atrophy. *Salmonella* Typhimurium, lipopolysaccharide (LPS), etoposide (Eto) and dexamethasone (Dex) induce severe thymic atrophy in BALB/c mice. LPS and Eto depletes all the major thymocyte subsets, *S. Typhimurium* specifically reduces the double-negative (DN) ( $CD4^- CD8^-$ ), immature single-positive (ISP) ( $CD4^- CD8^+ CD3^{lo} CD24^{hi}$ ) and double-positive (DP) ( $CD4^+ CD8^+$ ) cells, Dex decreases the DP and SP ( $CD4^+ CD8^- / CD4^- CD8^+$ ) cells. Eto- and Dex-induced thymic atrophy are reactive oxygen species (ROS) -independent (red lines), while *S. Typhimurium*- and LPS-induced thymic atrophy are ROS-dependent (blue lines).

thymocyte apoptosis *in vitro*, most likely through the inhibition of copper-mediated Fenton reactions.<sup>54</sup> During Dex-mediated thymic atrophy, thymocyte apoptosis occurs due to increased mitochondria-derived hydrogen peroxide and the antioxidant, NAC reduces cell death *in vitro* and *in vivo*.<sup>55</sup> In our study, *S. Typhimurium*- and LPS-induced thymic atrophy (both inflammatory models) were observed to be ROS-dependent (Fig. 7). Of note, NAC did reduce infection-induced cortisol amounts (Fig. 9d). Further studies are required to understand the mechanisms involved in the NAC-mediated increase in survival of thymic subsets during infection- and LPS-induced thymic atrophy.

Overall, there are two important points from this study. First, thymic subpopulations are differentially affected during various modes of atrophy. Some treatments (LPS and Eto) target all the major thymocyte subpopulations for depletion, but others (ST and Dex) display selectivity (Fig. 10). Second, it is unlikely that generic thymopoietic molecules that target the oxidative stress pathway will be effective against all modes of thymic atrophy. These results call for screening of molecules that will be effective against selective conditions of thymic atrophy, e.g. infections, transplantation, stress, etc. The study of the thymocyte subpopulations during atrophy

will facilitate the identification of superior thymopoietic molecules which may, in turn, boost the thymic output and aid in T-cell reconstitution under distinct conditions.

## Acknowledgements

SM and AR performed the experiments, SM, VA, AR, SRR and DN analysed the results, SM and DN designed the study, and SM and DN wrote the manuscript. The final draft of the manuscript was approved by all the authors. We appreciate the assistance of Dr William Surin, Dr Uttara Chakraborty, members of the IISc Bangalore Flow Cytometry Facility and also the past and present members of the DpN laboratory, IISc. We also acknowledge the Central Animal Facility of IISc for providing mice for this study. The financial assistance of a grant from SERB is greatly appreciated. In addition, we are grateful for the infrastructural resources provided by the DBT-IISc partnership, DST-FIST and UGC-SAP programmes.

## Disclosure

The authors declare no conflict of interest.

## References

- 1 Yui MA, Rothenberg EV. Developmental gene networks: a triathlon on the course to T cell identity. *Nat Rev Immunol* 2014; **14**:529–45.
- 2 Saini M, Pearson C, Seddon B. Regulation of T cell-dendritic cell interactions by IL-7 governs T-cell activation and homeostasis. *Blood* 2009; **113**:5793–800.
- 3 Kishimoto H, Sprent J. Negative selection in the thymus includes semimature T cells. *J Exp Med* 1997; **185**:263–71.
- 4 Rosen H, Alfonso C, Surh CD, McHeyzer-Williams MG. Rapid induction of medullary thymocyte phenotypic maturation and egress inhibition by nanomolar sphingosine 1-phosphate receptor agonist. *Proc Natl Acad Sci USA* 2003; **100**:10907–12.
- 5 Majumdar S, Deobagkar-Lele M, Adiga V, Raghavan A, Wadhwa N, Ahmed SM *et al*. Differential susceptibility and maturation of thymocyte subsets during *Salmonella* Typhimurium infection: insights on the roles of glucocorticoids and Interferon- $\gamma$ . *Sci Rep* 2017; **7**:40793.
- 6 Majumdar S, Nandi D. Thymic Atrophy: experimental Studies and Therapeutic Interventions. *Scand J Immunol* 2018; **87**:4–14.
- 7 Nunes-Alves C, Nobrega C, Behar SM, Correia-Neves M. Tolerance has its limits: how the thymus copes with infection. *Trends Immunol* 2013; **34**:502–10.
- 8 Wang SD, Huang KJ, Lin YS, Lei HY. Sepsis-induced apoptosis of the thymocytes in mice. *J Immunol* 1994; **152**:5014–21.
- 9 Billard MJ, Gruver AL, Sempowski GD. Acute endotoxin-induced thymic atrophy is characterized by intrathymic inflammatory and wound healing responses. *PLoS ONE* 2011; **6**:e17940.
- 10 Norimatsu M, Ono T, Aoki A, Ohishi K, Tamura Y. *In vivo* induction of apoptosis in murine lymphocytes by bacterial lipopolysaccharides. *J Med Microbiol* 1995; **43**:251–7.
- 11 Sempowski GD, Rhein ME, Scarse RM, Haynes BF. Leukemia inhibitory factor is a mediator of *Escherichia coli* lipopolysaccharide-induced acute thymic atrophy. *Eur J Immunol* 2002; **32**:3066–70.
- 12 Choyke PL, Zeman RK, Gootenberg JE, Greenberg JN, Hoffer F, Frank JA. Thymic atrophy and regrowth in response to chemotherapy: CT evaluation. *AJR Am J Roentgenol* 1987; **149**:269–72.
- 13 Hendrickx P, Döhning W. Thymic atrophy and rebound enlargement following chemotherapy for testicular cancer. *Acta Radiol* 1989; **30**:263–7.
- 14 Fearnhead HO, Chwalinski M, Snowden RT, Ormerod MG, Cohen GM. Dexamethasone and etoposide induce apoptosis in rat thymocytes from different phases of the cell cycle. *Biochem Pharmacol* 1994; **48**:1073–9.
- 15 Bustamante J, Bersier G, Badin RA, Cymeryng C, Parodi A, Boveris A. Sequential NO production by mitochondria and endoplasmic reticulum during induced apoptosis. *Nitric Oxide* 2002; **6**:333–41.

- 16 Sun XM, Carthew P, Dinsdale D, Snowden RT, Cohen GM. The involvement of apoptosis in etoposide-induced thymic atrophy. *Toxicol Appl Pharmacol* 1994; **128**:78–85.
- 17 Stefanelli C, Bonavita F, Stanic I, Pignatti C, Farruggia G, Masotti L et al. Inhibition of etoposide-induced apoptosis with peptide aldehyde inhibitors of proteasome. *Biochem J* 1998; **332**(Pt 3):661–5.
- 18 Marchetti MC, Di Marco B, Cifone G, Migliorati G, Riccardi C. Dexamethasone-induced apoptosis of thymocytes: role of glucocorticoid receptor-associated Src kinase and caspase-8 activation. *Blood* 2003; **101**:585–93.
- 19 Ito M, Nishiyama K, Hyodo S, Shigeta S, Ito T. Weight reduction of thymus and depletion of lymphocytes of T-dependent areas in peripheral lymphoid tissues of mice infected with *Francisella tularensis*. *Infect Immun* 1985; **49**:812–8.
- 20 Perry LL, Hotchkiss JD, Lodmell DL. Murine susceptibility to street rabies virus is unrelated to induction of host lymphoid depletion. *J Immunol* 1990; **144**:3552–7.
- 21 Chen W, Kuolee R, Austin JW, Shen H, Che Y, Conlan JW. Low dose aerosol infection of mice with virulent type A *Francisella tularensis* induces severe thymus atrophy and CD4<sup>+</sup> CD8<sup>+</sup> thymocyte depletion. *Microb Pathog* 2005; **39**:189–96.
- 22 Roggero E, Pérez AR, Tamae-Kakazu M, Piazzon I, Nepomnaschy I, Besedovsky HO et al. Endogenous glucocorticoids cause thymus atrophy but are protective during acute *Trypanosoma cruzi* infection. *J Endocrinol* 2006; **190**:495–503.
- 23 Deobagkar-Lele M, Chacko SK, Victor ES, Kadthur JC, Nandi D. Interferon- $\gamma$ - and glucocorticoid-mediated pathways synergize to enhance death of CD4<sup>+</sup> CD8<sup>+</sup> thymocytes during *Salmonella enterica* serovar Typhimurium infection. *Immunology* 2013; **138**:307–21.
- 24 Zhang YH, Takahashi K, Jiang GZ, Kawai M, Fukada M, Yokochi T. *In vivo* induction of apoptosis (programmed cell death) in mouse thymus by administration of lipopolysaccharide. *Infect Immun* 1993; **61**:5044–8.
- 25 Kato Y, Morikawa A, Sugiyama T, Koide N, Jiang GZ, Takahashi K et al. Role of tumor necrosis factor- $\alpha$  and glucocorticoid on lipopolysaccharide (LPS)-induced apoptosis of thymocytes. *FEMS Immunol Med Microbiol* 1995; **12**:195–204.
- 26 Kaiserlian D, Savino W, Hassid J, Dardenne M. Studies of the thymus in mice bearing the Lewis lung carcinoma III. Possible mechanisms of tumor-induced thymic atrophy. *Clin Immunol Immunopathol* 1984; **32**:316–25.
- 27 Prins RM, Graf MR, Merchant RE, Black KL, Wheeler CJ. Thymic function and output of recent thymic emigrant T cells during intracranial glioma progression. *J Neurooncol* 2003; **64**:45–54.
- 28 Deobagkar-Lele M, Victor ES, Nandi D. c-Jun NH<sub>2</sub>-terminal kinase is a critical node in the death of CD4<sup>+</sup>CD8<sup>+</sup> thymocytes during *Salmonella enterica* serovar Typhimurium infection. *Eur J Immunol* 2014; **44**:137–49.
- 29 Brewer JA, Sleckman BP, Swat W, Muglia LJ. Green fluorescent protein-glucocorticoid receptor knockin mice reveal dynamic receptor modulation during thymocyte development. *J Immunol* 2002; **169**:1309–18.
- 30 Liu D, Liu A. Administration of vitamin E prevents thymocyte apoptosis in murine sarcoma S180 tumor bearing mice. *Cell Mol Biol (Noisy-le-grand)* 2012; **58**(Suppl):OL1671–9.
- 31 Obukhova LA, Skulachev VP, Kolosova NG. Mitochondria-targeted antioxidant SkQ1 inhibits age-dependent involution of the thymus in normal and senescence-prone rats. *Aging (Albany NY)* 2009; **1**:389–401.
- 32 Scofield VL, Yan M, Kuang X, Kim S-J, Crunk D, Wong PKY. The drug monosodium luminol (GVT) preserves thymic epithelial cell cytoarchitecture and allows thymocyte survival in mice infected with the T cell-tropic, cytopathic retrovirus ts1. *Immunol Lett* 2009; **122**:159–69.
- 33 Uchio R, Hirose Y, Murosaki S, Yamamoto Y, Ishigami A. High dietary intake of vitamin C suppresses age-related thymic atrophy and contributes to the maintenance of immune cells in vitamin C-deficient senescence marker protein-30 knockout mice. *Br J Nutr* 2015; **113**:603–9.
- 34 Guevara Patiño JA, Marino MW, Ivanov VN, Nikolich-Zugich J. Sex steroids induce apoptosis of CD8<sup>+</sup> CD4<sup>+</sup> double-positive thymocytes via TNF- $\alpha$ . *Eur J Immunol* 2000; **30**:2586–92.
- 35 Hauri-Hohl MM, Keller MP, Gill J, Hafen K, Pachlatko E, Boulay T et al. Donor T-cell alloreactivity against host thymic epithelium limits T-cell development after bone marrow transplantation. *Blood* 2007; **109**:4080–8.
- 36 Borges M, Barreira-Silva P, Flório M, Jordan MB, Correia-Neves M, Appelberg R. Molecular and cellular mechanisms of *Mycobacterium avium*-induced thymic atrophy. *J Immunol* 2012; **189**:3600–8.
- 37 Liu B, Zhang X, Deng W, Liu J, Li H, Wen M et al. Severe influenza A(H1N1)pdm09 infection induces thymic atrophy through activating innate CD8<sup>+</sup>CD44<sup>hi</sup> T cells by upregulating IFN- $\gamma$ . *Cell Death Dis* 2014; **5**:e1440.
- 38 Duan X, Lu J, Zhou K, Wang J, Wu J, Gao GF et al. NK-cells are involved in thymic atrophy induced by influenza A virus infection. *J Gen Virol* 2015; **96**:3223–35.
- 39 Pérez AR, Roggero E, Nicora A, Palazzi J, Besedovsky HO, Del Rey A et al. Thymus atrophy during *Trypanosoma cruzi* infection is caused by an immuno-endocrine imbalance. *Brain Behav Immun* 2007; **21**:890–900.
- 40 Liepinsh DJ, Kruglov AA, Galimov AR, Shakhov AN, Shebzukhov YV, Kuchmiy AA et al. Accelerated thymic atrophy as a result of elevated homeostatic expression of the genes encoded by the TNF/lymphotoxin cytokine locus. *Eur J Immunol* 2009; **39**:2906–15.
- 41 Schilham MW, Wilson A, Moerer P, Benaissa-Trouw BJ, Cumano A, Clevers HC. Critical involvement of Tcf-1 in expansion of thymocytes. *J Immunol* 1998; **161**:3984–91.
- 42 Pellicciari C, Bottone MG, Schaack V, Barni S, Manfredi AA. Spontaneous apoptosis of thymocytes is uncoupled with progression through the cell cycle. *Exp Cell Res* 1996; **229**:370–7.
- 43 Porritt HE, Gordon K, Petrie HT. Kinetics of steady-state differentiation and mapping of intrathymic-signaling environments by stem cell transplantation in nonirradiated mice. *J Exp Med* 2003; **198**:957–62.
- 44 Berki T, Pálkás L, Boldizsár F, Németh P. Glucocorticoid (GC) sensitivity and GC receptor expression differ in thymocyte subpopulations. *Int Immunol* 2002; **14**:463–9.
- 45 Takigawa T, Miyazaki H, Kinoshita M, Kawarabayashi N, Nishiyama K, Hatsuse K et al. Glucocorticoid receptor-dependent immunomodulatory effect of ursodeoxycholic acid on liver lymphocytes in mice. *Am J Physiol Gastrointest Liver Physiol* 2013; **305**:G427–38.
- 46 Boldizsár F, Pálkás L, Czömpöly T, Bartis D, Németh P, Berki T. Low glucocorticoid receptor (GR), high Dig2 and low Bcl-2 expression in double positive thymocytes of BALB/c mice indicates their endogenous glucocorticoid hormone exposure. *Immunobiology* 2006; **211**:785–96.
- 47 Ozeki Y, Kaneda K, Fujiwara N, Morimoto M, Oka S, Yano I. *In vivo* induction of apoptosis in the thymus by administration of mycobacterial cord factor (trehalose 6,6'-dimycolate). *Infect Immun* 1997; **65**:1793–9.
- 48 MacDonald HR, Budd RC, Howe RC. A CD3<sup>+</sup> subset of CD4<sup>+</sup> 8<sup>+</sup> thymocytes: a rapidly cycling intermediate in the generation of CD4<sup>+</sup>8<sup>+</sup> cells. *Eur J Immunol* 1988; **18**:519–23.
- 49 Shortman K, Wilson A, Egerton M, Pearse M, Scollay R. Immature CD4<sup>+</sup>CD8<sup>+</sup> murine thymocytes. *Cell Immunol* 1988; **113**:462–79.
- 50 Ferreira BL, Ferreira ÉR, de Brito MV, Salu BR, Oliva MLV, Mortara RA et al. BALB/c and C57BL/6 mice cytokine responses to *Trypanosoma cruzi* infection are independent of parasite strain infectivity. *Front Microbiol* 2018; **9**:553.
- 51 Schlüter D, Deckert-Schlüter M, Lorenz E, Meyer T, Röllinghoff M, Bogdan C. Inhibition of inducible nitric oxide synthase exacerbates chronic cerebral toxoplasmosis in *Toxoplasma gondii*-susceptible C57BL/6 mice but does not reactivate the latent disease in *T. gondii*-resistant BALB/c mice. *J Immunol* 1999; **162**:3512–8.
- 52 Sawicka M, Stritesky GL, Reynolds J, Abourashchi N, Lythe G, Molina-Paris C et al. From pre-DP, post-DP, SP4, and SP8 thymocyte cell counts to a dynamical model of cortical and medullary selection. *Front Immunol* 2014; **5**:19.
- 53 Müller F, Svardal AM, Nordoy I, Berge RK, Aukrust P, Frøland SS. Virological and immunological effects of antioxidant treatment in patients with HIV infection. *Eur J Clin Invest* 2000; **30**:905–14.
- 54 Wolfe JT, Ross D, Cohen GM. A role for metals and free radicals in the induction of apoptosis in thymocytes. *FEBS Lett* 1994; **352**:58–62.
- 55 Tonomura N, McLaughlin K, Grimm L, Goldsby RA, Osborne BA. Glucocorticoid-induced apoptosis of thymocytes: requirement of proteasome-dependent mitochondrial activity. *J Immunol* 2003; **170**:2469–78.

## Supporting Information

Additional Supporting Information may be found online in the Supporting Information section at the end of the article:

**Figure S1.** Dexamethasone and etoposide, at low concentrations, directly induce *in vitro* thymocyte death. Thymocytes from 6- to 8-week-old male BALB/c mice were obtained and seeded at a density of 500 000 cells per well in 96-well U-bottomed plates.

**Figure S2.** N-Acetyl cysteine (NAC) administration rescues the depletion of double-negative and double positive thymocytes during *Salmonella* Typhimurium- and lipopolysaccharide-mediated thymic atrophy.

**Figure S3.** The double-negative and double-positive subsets are rescued after N-acetyl cysteine treatment during infection and lipopolysaccharide-induced thymic atrophy.

**Figure S4.** Depletion of immature single-positive cells during infection- and lipopolysaccharide-induced thymic atrophy is reactive oxygen species-dependent.

**Table S1.** Comparison of the significant changes occurring in the thymi of the two mouse strains, C57BL/6 and BALB/c after *Salmonella* Typhimurium infection.